X-ray structure of a putative reaction intermediate of 5-aminolaevulinic acid dehydratase

Peter T. ERSKINE*, Leighton COATES*, Danica BUTLER*, James H. YOUELL*, Amanda A. BRINDLEY†, Steve P. WOOD*, Martin J. WARREN†, Peter M. SHOOLINGIN-JORDAN* and Jonathan B. COOPER*[1]

*Division of Biochemistry and Molecular Biology, School of Biological Sciences, University of Southampton, Bassett Crescent East, Southampton, SO16 7PX, U.K., and †School of Biological Sciences, Queen Mary, Mile End Road, London, E1 4NS, U.K.

The X-ray structure of yeast 5-aminolaevulinic acid dehydratase, in which the catalytic site of the enzyme is complexed with a putative cyclic intermediate composed of both substrate moieties, has been solved at 0.16 nm (1.6 Å) resolution. The cyclic intermediate is bound covalently to Lys[263] with the amino group of the aminomethyl side chain ligated to the active-site zinc ion in a position normally occupied by a catalytic hydroxide ion. The cyclic intermediate is catalytically competent, as shown by its turnover in the presence of added substrate to form porphobilinogen. The findings, combined with those of previous studies, are consistent with a catalytic mechanism in which the C–C bond linking both substrates in the intermediate is formed before the C–N bond.

Key words: 5-aminolaevulinic acid dehydratase, catalytic mechanism, reaction intermediate, trapped intermediate, X-ray structure.

INTRODUCTION

The enzyme 5-aminolaevulinic acid dehydratase [ALAD; porphobilinogen (PBG) synthase, E.C. 4.2.1.24] catalyses an early step in the biosynthesis of tetrapyrroles involving the condensation of two 5-aminolaevulinic acid (ALA) molecules to form the pyrrole PBG (see Scheme 1) [1–5]. Subsequent enzymes in the pathway cyclize four of these PBG molecules to make the core tetrapyrrole framework uroporphyrinogen III, which undergoes various modifications to form a variety of essential metallo-prosthetic groups, including haem, chlorophyll and the cobalamins. ALADs share a high degree of sequence identity, contain about 350 amino acids per subunit and are usually octameric. In humans, hereditary deficiencies in ALAD give rise to the rare disease Doss porphyria [6], and the exquisite sensitivity of the human enzyme to inhibition by lead ions is a major factor in acute lead poisoning [7,8].

The structures of ALADs from several species have been determined, and several inhibitor complexes have been studied [9–12]. In these structures the enzyme is a homo-octamer with each subunit adopting a $(\beta/\alpha)_8$ or TIM (triosephosphate isomerase) barrel fold with an N-terminal arm which, in yeast ALAD, is 39 residues in length (Figure 1). Within the octamer, subunits form dimers in which each subunit has its N-terminal arm wrapped around the barrel of the other monomer. The active site of each subunit is located in a pronounced cavity formed by loops at the C-terminal ends of the β-strands forming the TIM barrel. All eight active sites are oriented towards the outer surface of the octamer and are independent.

At the base of each active site are two lysine residues (Lys[210] and Lys[263] in yeast ALAD), one of which (Lys[263]) is known to form a Schiff-base link to the first molecule of substrate that binds to the active site [13,14]. The substrate bound to Lys[263] is incorporated into the propionic acid side, or P-side, of the product PBG whereas the second substrate molecule forms the acetic acid side, or A-side, of PBG (see Scheme 1). Thus catalysis proceeds by fo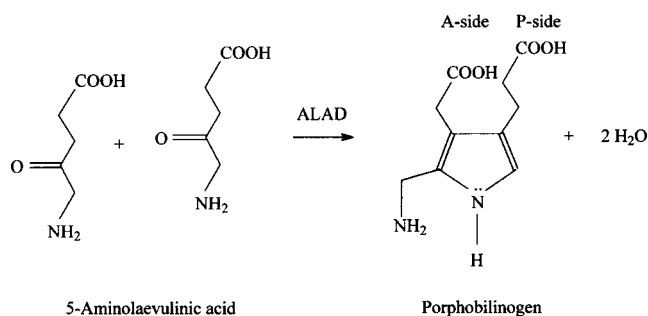rmation of a Schiff-base link at the P-site between the 4-oxo group of substrate ALA and an invariant lysine residue, equivalent to Lys[263] in yeast ALAD. In many ALADs, an active-site zinc ion has been implicated in the catalytic mechanism and is thought to act on substrate bound to the A-site. The zinc-binding site is formed by the following residues in yeast ALAD: Cys[133], Cys[135] and Cys[143]. In contrast, the plant and some bacterial ALADs require magnesium and lack the triple-cysteine sequence motif, which is replaced by two aspartate residues and an alanine residue [15]. A more detailed characterization of the metal requirement of ALADs is given in [5].

Previously, the structures ALADs in which the P-site is occupied by a number of bound inhibitors have been analysed, and the structure of substrate ALA bound in this site has also been determined [16]. All ligands form a Schiff base with Lys[263] and are held with their carboxy groups making hydrogen bonds with the conserved residues Ser[290] and Tyr[329]. Hydrophobic interactions are made with the side chains of residues Tyr[216], Phe[219], Tyr[287] and Val[289], which effectively form four sides of this substrate-binding subsite. In yeast ALAD, ALA appears to bind in two conformations, but in both of these conformers the C-5 amino group interacts with the side chains of Asp[131] and Ser[179]. This implicates these two residues as having potential catalytic roles in the reaction mechanism. The A-site is a solvent-filled cavity bounded on one side by the P-site ALA molecule and on the other by two arginine residues (Arg[220] and Arg[232]) which are strongly conserved. The base of the A-site is formed by the zinc ion held by three cysteine residues. There is a solvent molecule bound to the zinc ion which is within H-bonding distance of the amino group of P-side ALA. This water molecule may be a zinc-bound hydroxide which abstracts a proton from C-3 of A-side ALA as a prerequisite for formation of the C–C bond between the two substrates.

Hitherto, mechanistic proposals for ALAD have been dominated by the experimental finding that the enzyme only forms a Schiff base with one of the two identical substrate molecules. This was based on labelling studies which showed only

Scheme 1   Reaction catalysed by ALAD

this inhibitor forms two Schiff bases at the active site, involving Lys[210] as well as Lys[263]. One half of the molecule resides in the P-site and the other half fills the putative A-site with its carboxy group interacting with invariant arginine residues Arg[220] and Arg[232] The structure of *Pseudomonas aeruginosa* ALAD complexed with 5-fluorolaevulinic acid [19] shows that both A- and P-sites are occupied by an inhibitor molecule covalently bound through a Schiff base with Lys[210] and Lys[263] respectively. The structural evidence that both invariant lysine residues may form Schiff bases with substrate at the active site is suggestive of a double-Schiff-base mechanism such as that proposed by Neier [20].

Previously, we found that ALA was covalently bound as a Schiff base to Lys[263] at the P-site of yeast ALAD, despite the fact that ALA had not been added to the enzyme [16]. It has also been observed that human ALAD, highly purified from erythrocytes, possesses a ligand resembling PBG at the active site, despite the fact that no ligands had been externally added [12]. In the present study we have found that crystallizing the purified yeast dehydratase in the presence of added 5-aminolaevulinic acid results in the trapping of what appears to be a similar cyclic intermediate complex, arising from the reaction of two substrate molecules at the active site. The intermediate is catalytically competent and can turn over to form the product, PBG. The complex, refined at 0.16 nm (1.6 Å) resolution, shows a covalent link between Lys[263] and the intermediate, a direct link with the zinc ion and provides important stereochemical information giving an unprecedented view of active-site interactions. A catalytic mechanism taking into account the structure of the enzyme–intermediate complex is proposed.

EXPERIMENTAL

Recombinant yeast ALAD was purified as described previously [9]. Crystals of yeast ALAD with the bound intermediate were obtained by co-crystallizing the enzyme in the presence of substrate (ALA). The hanging-drop vapour-diffusion method was used with ALA present at a concentration of 0.2 mM and enzyme present at a concentration of 2 mg/ml. Apart from the presence of ALA, the crystallization conditions [2–10 % (w/v) poly(ethylene glycol) of molecular mass 6000 Da/200 mM Tris/HCl, pH range 7.0 – 8.0] are otherwise identical with those used to crystallize the native enzyme [21]. Crystals of the complex, which appeared within 3–4 weeks, belong to space group I422 with unit cell parameters of $a = b = 10.32$ nm (103.2 Å), $c = 16.7$ nm (167.7 Å). The crystals were flash-cooled in liquid ethane and X-ray data were collected at the European Synchrotron Radiation Facility (ESRF; Grenoble, France) using the ID-29 beam line with the crystal maintained at a temperature of 100 K using an Oxford Cryosystems (Long Hanborough, Oxford, U.K.) cooler. The data were processed using MOSFLM [22] and the CCP4 suite [23]. The structure was refined using SHELX [24] and the program RESTRAIN [25] was used for refinement of translation-libration-screw (TLS) tensors. Graphical rebuilding was done using TURBO-FRODO (Bio-Graphics, Marseille, France) running on Silicon-Graphics (SGI) computers. The co-ordinates and structure factors have been deposited in the Protein Data Bank with accession codes 1ohl and r1ohlsf respectively.

RESULTS AND DISCUSSION

Interpretation of the electron-density difference map

The initial difference map for yeast ALAD co-crystallized with ALA showed strong electron density for a five-membered ring
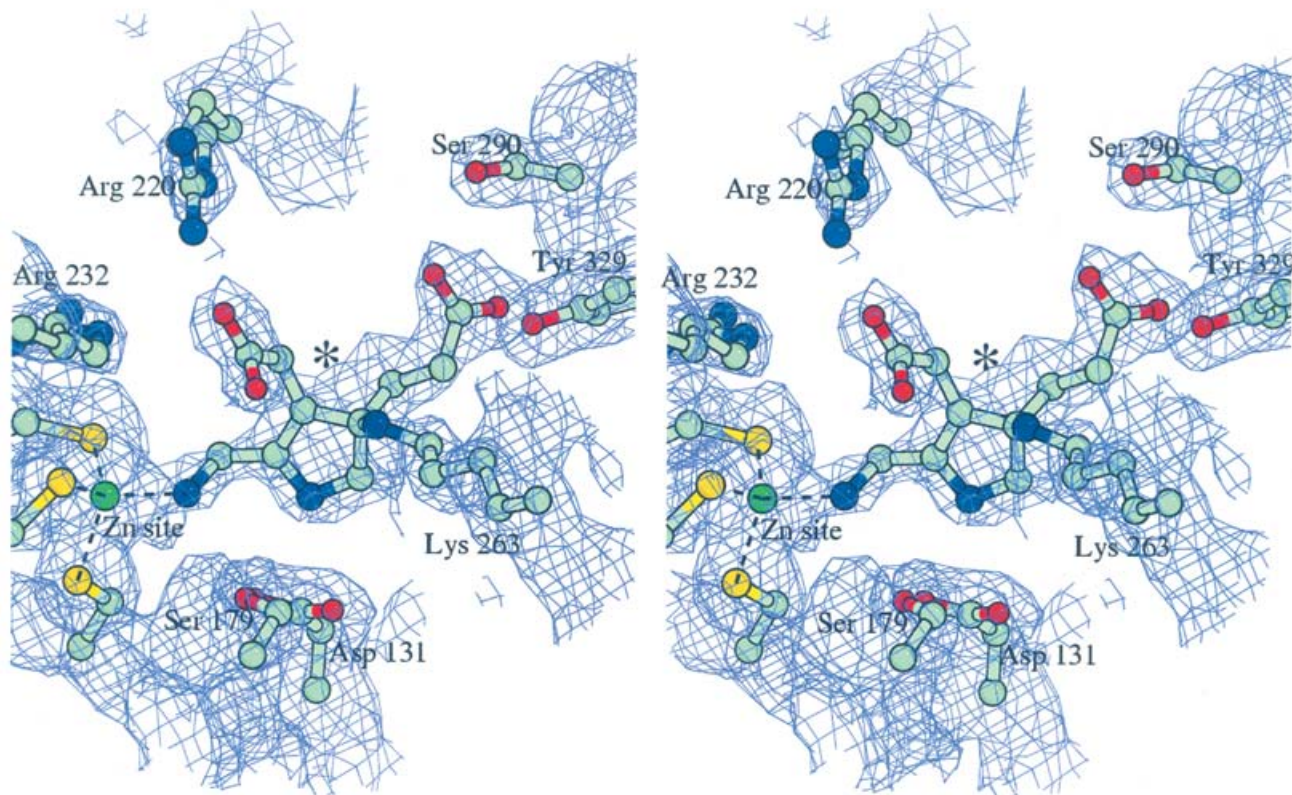

Figure 1   Tertiary structure of a monomer of yeast ALAD showing the active-site Lys[263] along with the bound intermediate in ball-and-stick representation

The zinc ion is also shown (the larger, separate, black sphere). Residues 213–233 over the active site are omitted in order to show the position of the putative intermediate more clearly.

the P-side substrate becoming covalently trapped upon reduction with NaBH$_4$ [13,14]. Recently, the structures of the yeast and *Escherichia coli* enzymes complexed with the irreversible inhibitor 4,7-dioxosebacic acid have been solved [17,18]. Intriguingly

Figure 2   Stereo view of the electron-density map of the putative intermediate (labelled *) covalently bound to Lys[263] at 0.16 nm (1.6 Å) resolution

The map was weighted as described by Read [32], and is contoured at 1.0 root mean square. The P-site is on the right-hand side and the A-site is formed by residues shown on the left-hand side including the zinc ion. The other invariant lysine (Lys[210]) is in the foreground just to the left of Lys[263], but it has been omitted for clarity. The side chains of the two lysine residues lie approximately parallel with each other.

intermediate resembling PBG bound to Lys[263] in the active site. The ligand was built into the density accordingly and the structure of the complex refined for several cycles after each round of manual rebuilding. The refined electron-density maps at 0.16 nm (1.6 Å) resolution established that the carbon atoms of the five-membered ring to which the acetic acid and propionic acid groups are attached were trigonal. The final electron-density map is shown in Figure 2. Refinement of the occupancy of the ligand yielded a value of 81 % confirming that the putative intermediate has been trapped in the majority of the enzyme molecules forming the crystal. The atoms of the bound intermediate have a mean isotropic B-factor (B_{iso}) of 0.4 nm^2 (40.0 Å^2), which is comparable with the B-factors of the entire complex [mean $B_{iso} = 0.383$ nm^2 (38.3 Å^2)]. This presumably reflects on the buried state of the ligand, which is covered by the enzyme's active-site flap (residues 215–235).

The final structure, which has been refined using data between 4.5 nm (45 Å) and 0.16 nm (1.6 Å), has an R-factor of 18.8 % and an R-free of 24.1 % (see Table 1). Refinement of the TLS tensors for the TIM barrel and arm domains gave a significant improvement in R-free of over 7 %. The structure has 90.8 % of its residues within the 'most favoured' regions of the Ramachandran plot by the PROCHECK criteria [26] and 8.6 % of residues within the so-called 'additional allowed' boundary. No residues are in the disallowed regions. The temperature factors are reasonable, except for a few residues in the active-site flap (most notably 228–230), where the electron density remains poor despite extensive efforts to rebuild these residues throughout the refinement process.

Table 1   X-ray statistics for the complex of yeast ALAD with the putative intermediate after TLS refinement

Abbreviation: RMSD, root-mean-square deviation.

Parameter	Value
Statistics for entire dataset	
Resolution range [nm (Å)]	4.47–0.16 (44.7–1.6)
R_{merge} (%)	5.5
Completeness (%)	96.2
Multiplicity	7.2
Mean $I/\sigma(I)$	21.7
%$I > 3\sigma(I)$	77.5
Statistics for outer shell	
Resolution range [nm (Å)]	0.17–0.16 (1.7–1.6)
R_{merge} (%)	38.8
Completeness (%)	96.2
Multiplicity	2.6
Mean $I/\sigma(I)$	2.5
Refinement	
R-factor (%)	18.8
R-free (%)	24.1
Number of reflections	57 545
RMSD bond lengths [nm (Å)]	0.0005 (0.005)
RMSD 1–3 distances [nm (Å)]	0.0013 (0.013)
RMSD bumps [nm (Å)]	0.0015 (0.015)
RMSD chiral tetrahedra [nm (Å)]	0.0009 (0.009)
RMSD main-chain planes [nm (Å)]	0.0009 (0.009)
RMSD side-chain planes [nm (Å)]	0.0007 (0.007)

Nonetheless the electron density for the active-site loop in this complex is substantially better than that of the native enzyme.

Interactions made by the putative intermediate

The active site of ALAD is located in a large cavity at the C-terminal end of the eight-stranded all-parallel β-barrel (Figure 1). It involves two invariant lysine residues (Lys[263] and Lys[210] in yeast ALAD) as well as a zinc ion which is co-ordinated by three cysteine residues (Cys[133], Cys[135] and Cys[143]) in the yeast enzyme.

The trapped intermediate is held by a covalent bond to the invariant lysine residue in the P-site, namely Lys[263] (Figure 2). The P-side of the intermediate is surrounded by the hydrophobic side chains of Tyr[216], Phe[219], Tyr[287] and Val[289]. The P-side carboxy group forms hydrogen bonds with the side chains of Ser[290] and Tyr[329] and the P-side amino group is close to the side chains of Ser[179] and Asp[131]. The side chains of Phe[89] and Tyr[207] are also involved in forming this binding site. All of the above residues are invariant or strongly conserved, implying an important role for them in substrate binding to ALADs from all species. The putative intermediate defined in this analysis makes essentially the same interactions on its P-side as a number of inhibitors which occupy the P-site only [10,11,16,27]. The analysis confirmed that the intermediate is not bound covalently to the other active-site lysine residue (Lys[210]), even though this has been shown to make a Schiff base in complexes with inhibitors that occupy the A-site [17–19].

In previous studies of inhibitor and substrate binding at the P-site alone [10,11,16,27], the location of the A-site of ALAD was inferred from the presence of a solvent-filled cavity adjacent to the P-site ligand. This cavity is formed by the zinc ion and a number of invariant residues, including Arg[220], Arg[232] and Gln[236]. These predictions are largely confirmed by the currently determined structure in which it was found that the arginine side chains make electrostatic interactions with the A-side carboxy group (Figure 2). This was also found in the bound structure of the inhibitor 4,7-dioxosebacic acid, which occupies the A- and P-sites [17–18]. However, in the structure of the putative intermediate there is an additional interaction between the A-side carboxyl group and the side-chain amino group of Lys[210] – one of the two invariant catalytic lysine residues. It was speculated that the zinc ion plays an important mechanistic role by interacting with the A-side ALA via a solvent molecule which is bound datively to the metal ion. The requirement for a base in the mechanism to abstract hydrogen atoms from the C-3 of A-side ALA suggests that the zinc-bound solvent molecule is a hydroxide ion. In the presently determined complex, the putative hydroxide ion appears to be substituted by the A-side amino group of the trapped intermediate, which binds datively to the metal ion.

Implications for the mechanism

Various mechanisms for ALAD based on the X-ray structures of bound ligands have been proposed (e.g. [10]). These relied on the experimental finding that only one of the substrate moieties (P-side ALA) forms a Schiff base with one of the active-site lysines (Lys[263] in yeast ALAD) [13,14]. However, the recent findings that A-side ALA may also bind by forming a Schiff base with Lys[210] [17–19] suggest that proposals for the mechanism need to be reconsidered accordingly.

Another major issue of discussion with regard to the ALAD mechanism has been the order in which the bonds linking the two ALA molecules are formed, i.e. whether C–C bond formation occurs before or after C–N bond formation. The structure of the putative intermediate reported here indicates that A-side ALA must be in contact with the putative zinc-bound hydroxide, a strongly basic group which could act on the C-3 carbon of the A-side substrate. The formation of a Schiff base between this ALA moiety and Lys[210] would further help to labilize the C-3 hydrogen atoms of A-side ALA and assist deprotonation of this carbon atom, yielding a bound enamine (see Scheme 2). This could lead to nucleophilic attack of the enamine at the A-site on the C-4 of P-side ALA, thus forming the C–C bond linking the substrates. The inter-substrate C–N bond then forms followed by the second deprotonation of the C-3 of A-side ALA, thereby yielding the intermediate found in the crystal structure (labelled '*' in Scheme 2). Although it is possible that the C–N bond could form first, thus yielding a Schiff base linking both substrates, this would imply that the Schiff base between A-side ALA and Lys[210] observed in recent studies [17–19] has no role in catalysis other than perhaps to anchor the A-side substrate prior to catalysis. If instead it is assumed that the Schiff base linking A-side ALA with Lys[210] has a catalytic function (rather than just a passive binding role), then it is likely that inter-substrate C–C bond formation would occur before the C–N bond formation, as shown in Scheme 2.

In the catalytic reaction, the putative zinc-bound hydroxide is likely to deprotonate the C-3 of A-side ALA [shown as base B(1) in Scheme 2]. The fact that this hydroxide is apparently displaced by the C-5 amino group of A-side ALA, which binds to the zinc instead, may contribute to the stability of the trapped intermediate. Previous NMR studies using isotopically labelled PBG have suggested that the amino group of the reaction product binds to the active-site zinc ion [28]. Two invariant residues, Asp[131] and Ser[179], which are likely to catalyse various proton transfers in the reaction, are shown in Figure 2 below the putative intermediate. Two potential catalytic roles for these residues [shown as bases B(2) and B(3) in Scheme 2] could include deprotonation of the P-side C-5 amino group and proton transfer to the amino group of Lys[210]. The fact that the side chains of Lys[210] and Lys[263] are adjacent would allow one to transfer a proton to the other during the reaction. For example, the base [labelled B(4) in Scheme 2] which protonates Lys[263] to facilitate breakdown of the putative intermediate could be Lys[210].

The apparent stability of the postulated intermediate, under conditions where no particular attempts have been made to trap it, begs the question of how it is stabilized in the crystal structure. Although it is possible that crystal packing contributes in some way to its stabilization, we believe that the intermediate may actually represent a *bona fide* step in the catalytic cycle that is awaiting the completion of the final stages of the catalytic mechanism (last three stages in Scheme 2). This premise is supported by preliminary observations that enzyme, allowed to turn over in the presence of [4-^{14}C]ALA, results in ^{14}C-labelled enzyme in which two substrate-equivalents are bound per subunit [29]. Addition of unlabelled ALA to the labelled enzyme results in the release of [^{14}C]PBG and generates unlabelled enzyme, presumably with the same (although unlabelled) intermediate at the active site. This is further supported by the observation from MS (N. Mills-Davies, D. Butler and P. M. Shoolingin-Jordan, unpublished work) that the human enzyme forms a stable complex in solution with a molecule of mass close to that of enzyme-bound PBG. In all cases, the enzyme intermediate complex is Ehrlich's-reagent-negative [30], indicating that the bound intermediate does not have the same chemical properties as PBG. The X-ray crystallography and biochemical studies are thus mutually reinforcing.

A further interesting observation arising from the X-ray analysis of the enzyme–ligand complex is that the high resolution of

Scheme 2.

A-SITE   **P-SITE**
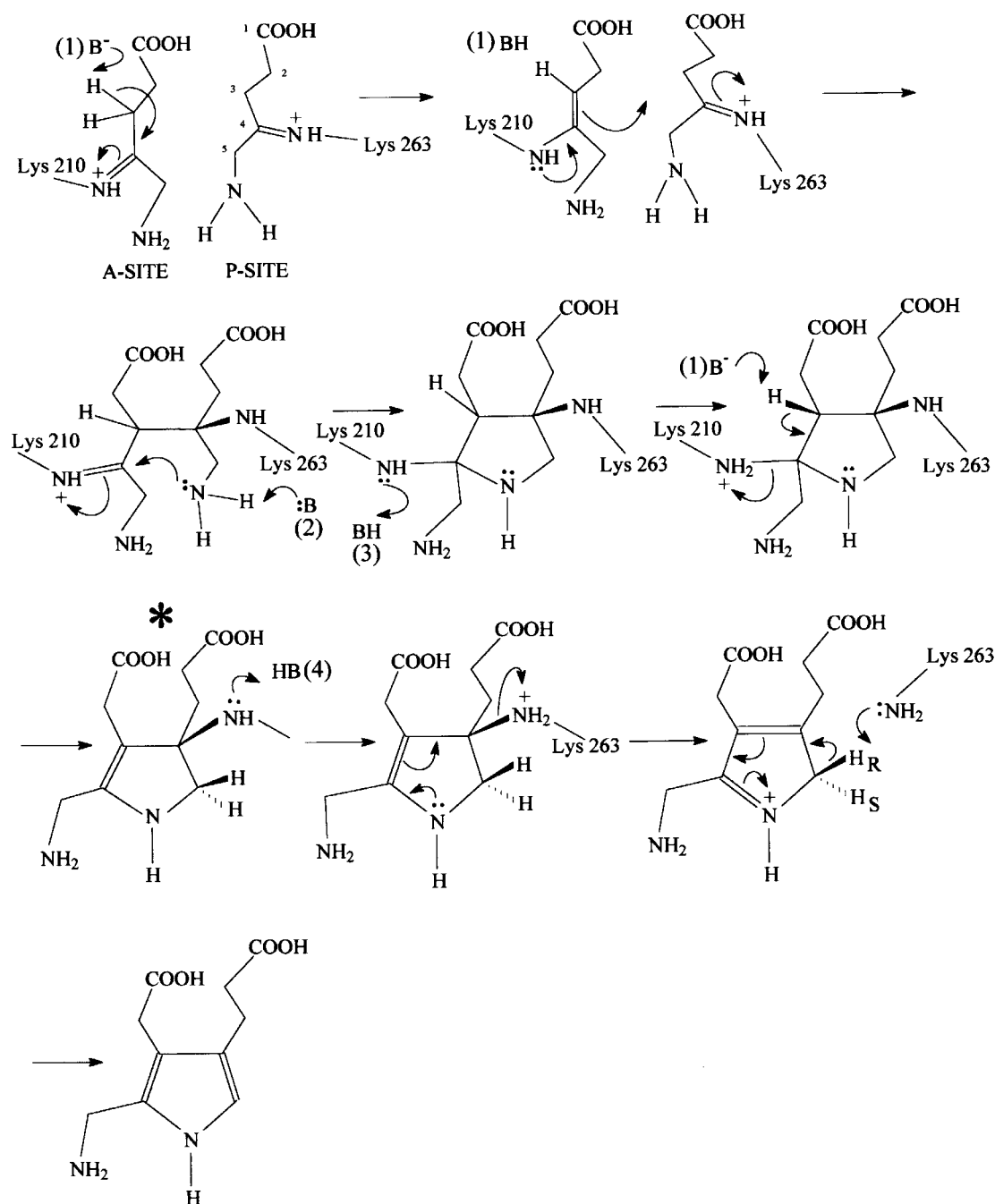
Scheme 2   Proposed mechanism for ALAD

It is assumed that the Schiff base made by Lys[210] with A-side ALA facilitates proton abstraction at its C-3 position. This leads to nucleophilic attack on P-side ALA forming the first C–C bond linking the substrates. The inter-substrate C–N bond then forms, yielding the putative intermediate found in the crystal structure (labelled *). Base (1)B is likely to be the putative zinc-bound hydroxide.

the structure allows the stereochemistry of the only chiral centre in the intermediate, the 3-position which is attached to Lys[263], to be assigned as *S*. Following the cleavage of the bond between Lys[263], the same lysine residue is in the optimal position to remove stereospecifically the proton from the 2-position (that becomes the free *a*-position) [31] and to complete the enzymic synthesis. The precise mechanism by which added substrate facilitates these last stages that culminate in the transformation of the bound intermediate into PBG is currently under detailed investigation.

REFERENCES

1   Jordan, P. M. (1991) Biosynthesis of tetrapyrroles. New Compr. Biochem. **19**, 1–65

2   Jordan, P. M. (1994) Highlights in haem biosynthesis. Curr. Opin. Struc. Mol. Biol. **4**, 902–911

3   Warren, M. J. and Scott, A. I. (1990) Tetrapyrrole assembly and modification into the ligands of biologically functional cofactors. Trends Biochem. Sci. **15**, 486–491

4   Jaffe, E. K. (1995) Porphobilinogen synthase, the first source of heme's asymmetry. J. Bioenerg. Biomembr. **27**, 169–179

5   Jaffe, E. K. (2003) Unusual phylogenetic variation in the metal ion binding sites of porphobilinogen synthase. Chem. Biol. **10**, 25–34

6   Doss, M., Von-Tieperman, R., Schneider, J. and Schmid, H. (1979) New types of hepatic porphyria with porphobilinogen synthase defect and intermittent acute clinical manifestation. Klin. Wochenschr. **57**, 1123–1127

7   Simons, T. J. B. (1995) The affinity of human erythrocyte porphobilinogen synthase for Zn^{2+} and Pb^{2+}. Eur. J. Biochem. **234**, 178–183

8   Warren, M. J., Cooper, J. B., Wood, S. P. and Shoolingin-Jordan, P. M. (1998) Lead poisoning, haem synthesis and 5-aminolevulinic acid dehydratase. Trends Biochem. Sci. **23**, 217–221

9   Erskine, P. T., Senior, N., Awan, S., Lambert, R., Lewis, G., Tickle, I. J., Sarwar, M., Spencer, P., Thomas, P., Warren, M. J., Shoolingin-Jordan, P. M. et al. (1997) X-ray structure of 5-aminolevulinate dehydratase, a hybrid aldolase. Nat. Struct. Biol. **4**, 1025–1031

10 Erskine, P. T., Norton, E., Cooper, J. B., Lambert, R., Coker, A., Lewis, G., Spencer, P., Sarwar, M., Wood, S. P., Warren, M. J. and Shoolingin-Jordan, M. J. (1999) The X-ray structure of 5-aminolevulinic acid dehydratase from *Escherichia coli* complexed with the inhibitor levulinic acid at 2.0 Å resolution. Biochemistry **38**, 4266–4276

11 Frankenberg, N., Erskine, P. T., Cooper, J. B., Shoolingin-Jordan, P. M., Jahn, D. and Heinz, D. W. (1999) High resolution crystal structure of a Mg^{2+}-dependent porphobilinogen synthase. J. Mol. Biol. **289**, 591–602

12 Mills-Davies, N. L. (2001) Structure of human erythrocyte 5-aminolaevulinic acid dehydratase, the second enzyme in the biosynthesis of haem. Ph.D. Thesis, University of Southampton

13 Jordan, P. M. and Gibbs, P. N. B. (1985) Mechanism of action of 5-aminolevulinate dehydratase from human erythrocytes. Biochem. J. **227**, 1015–1020

14 Gibbs, P. N. B. and Jordan, P. M. (1986) Identification of a lysine at the active site of human 5-aminolevulinate dehydratase. Biochem. J. **236**, 447–451

15 Boese, Q. F., Spano, A. J., Li, J. and Timko, M. P. (1991) 5-Aminolevulinic acid dehydratase in pea. Identification of an unusual metal-binding domain in the plant enzyme. J. Biol. Chem. **266**, 17060–17066

16 Erskine, P. T., Newbold, R., Brindley, A. A., Wood, S. P, Shoolingin-Jordan, P. M., Warren, M. J. and Cooper, J. B. (2001) The X-ray structure of yeast 5-aminolaevulinic acid dehydratase complexed with substrate and three inhibitors. J. Mol. Biol. **312**, 133–141

17 Erskine, P. T., Coates, L., Newbold, R., Brindley, A. A., Stauffer, F., Wood, S. P., Warren, M. J., Cooper, J. B., Shoolingin-Jordan, P. M. and Neier, R. (2001) The X-ray structure of yeast 5-aminolaevulinic acid dehydratase complexed with two diacid inhibitors. FEBS Lett. **503**, 196–200

18 Kervinen, J., Jaffe, E. K., Stauffer, F., Neier, R., Wlodawer, A., Zdanov, A. (2001) Mechanistic basis for suicide inactivation of porphobilinogen synthase by 4,7-dioxosebacic acid, an inhibitor that shows dramatic species selectivity. Biochemistry **40**, 8227–8236

19 Frère, F., Schubert, W.-D., Stauffer, F., Frankenberg, N., Neier, R., Jahn, D. and Heinz, D. W. (2002) Structure of porphobilinogen synthase from *Pseudomonas aeruginosa* in complex with 5-fluorolevulinic acid suggests a double Schiff base mechanism. J. Mol. Biol. **320**, 237–247

20 Neier, R. (1996) Chemical synthesis of porphobilinogen and studies of its biosynthesis. Adv. Nitrogen Heterocycl. **2**, 35–146

21 Erskine, P. T., Senior, N., Maignan, S., Cooper, J., Lambert, R., Lewis, G., Spencer, P., Awan, S., Warren, M., Tickle, I. J. et al. (1997) Crystallisation of 5-aminolevulinic acid dehydratase from *Escherichia coli* and *Saccharomyces cerevisiae* and preliminary X-ray characterisation of the crystals. Protein Sci. **6**, 1774–1776

22 Leslie, A. G. W. (1992) Recent changes to the MOSFLM package for processing film and image plate data. Joint CCP4+ESF-EAMCB Newsletter on Protein Crystallography, No. 26, Daresbury Laboratories, Warrington, U.K.

23 CCP4 (1994) The CCP4 suite: programs for protein crystallography. Acta Crystallogr. **D50**, 760–763

24 Sheldrick, G. M. and Schneider, T. R. (1997) SHELXL: high-resolution refinement. Methods Enzymol. **277**, 319–343

25 Haneef, I., Moss, D. S., Stanford, M. J. and Borkakoti, N. (1985) Restrained structure-factor least-squares refinement of protein structures using a vector-processing computer. Acta Crystallogr. **A41**, 426–433

26 Laskowski, R. A., MacArthur, M. W., Moss, D. S. and Thornton, J. M. (1993) PROCHECK: a program to check the stereochemical quality of protein structures. J. Appl. Crystallogr. **26**, 283–291

27 Erskine, P. T., Newbold, R., Roper, J., Coker, A., Warren, M. J., Shoolingin-Jordan, P. M., Wood, S. P. and Cooper, J. B. (1999) The Schiff base complex of yeast 5-aminolaevulinic acid dehydratase with laevulinic acid. Protein Sci. **8**, 1250–1256

28 Jaffe, E. K., Markham, G. D. and Rajogopalan, J. S. (1990) N-15 and C-13 NMR-studies of ligands bound to the 280,000-Dalton protein porphobilinogen synthase elucidate the structures of enzyme-bound product and a Schiff-base intermediate. Biochemistry **29**, 8345–8350

29 Butler, D. (2003) Characterisation and crystallisation of human 5-aminolaevulinic acid dehydratase and porphobilinogen deaminase. Ph.D. Thesis, University of Southampton

30 Mauzerall, D. and Granick, S. (1956) The occurrence and determination of δ-aminolevulinic acid and porphobilinogen in urine. J. Biol. Chem. **219**, 435–446

31 Chaudhry, A. G. and Jordan, P. M. (1976) Stereochemical studies on the formation of porphobilinogen. Biochem. Soc. Trans. **4**, 760–761

32 Read, R. J. (1986) Improved Fourier coefficients for maps using phases from partial structures with errors. Acta Crystallogr. **A42**, 140–149